Available online at www.sciencedirect.com
ScienceDirect
ELSEVIER
International Journal of Solids and Structures 44 (2007) 4167–4183
INTERNATIONAL JOURNAL OF SOLIDS and STRUCTURES
www.elsevier.com/locate/ijsolstr

In-plane stress analysis of an orthotropic plane containing multiple defects

A.R. Fotuhi, S.J. Fariborz *

Department of Mechanical Engineering, Amirkabir University of Technology (Tehran Polytechnic), 424, Hafez Avenue, Tehran 158754413, Iran

Received 9 July 2006; received in revised form 21 October 2006
Available online 15 November 2006

Abstract

The solution of Volterra type climb and glide edge dislocations is utilized to formulate integral equations for an orthotropic homogeneous infinite plane weakened by multiple smooth cracks and/or cavities. Cavities are considered as closed curved cracks without singularity. The integral equations are of Cauchy singular type which are converted to hypersingular integral equations. These equations are then solved numerically to determine stress intensity factors for cracks and hoop stress on the cavities. The results for isotropic and orthotropic planes are compared with available solutions in literature and excellent agreement is observed. The formulation allows stress analysis of orthotropic planes with several arbitrarily oriented cracks and cavities.

Keywords: Orthotropic plane; Elliptical cavity; Stress intensity factor; Hoop stress; Hypersingular integral equation

1. Introduction

The stress analysis in the presence of cracks and cavities is the vital part of damage assessment in the course of service life of structures weakened by these defects. The non-uniform distribution and variance in configuration of interacting defects pose quite a complicated stress analysis problem. Apparently the earliest attempt to analyze an infinite plane perforated by a uniform row of interacting circular holes dates back to the work of Howland (1935). Since the appearance of Howland's article, a significant number of papers dealing with the stress analysis in different regions containing cracks and cavities utilizing analytical and numerical approaches have been published. A few analytical investigations, not necessarily the most notable ones, are mentioned here. An infinitely long strip under tension weakened by two collinear equal circular holes situated on the center-line of strip was treated by Atsumi (1956). Haddon (1967) adopted the complex variable and conformal mapping techniques to analyze the problem of two interacting unequal circular holes, in an isotropic infinite plane. Isida (1973) employed the Laurent series expansion of complex potentials involving in the Airy stress

* Corresponding author. Tel.: +98 21 6454 3460; fax: +98 21 641 9736.
E-mail address: sjfariborz@yahoo.com (S.J. Fariborz).

0020-7683/$ - see front matter
doi:10.1016/j.ijsolstr.2006.11.020

function of an isotropic plane with elliptical holes. Cracks were considered as a limiting case of elliptical holes. The coefficients of the series were obtained via a perturbation procedure. The article, among other findings, analyzed the interaction of cracks and a crack with two holes. A complex body force density on the boundary of a hole was introduced by Duan et al. (1986). The application of boundary conditions on the surfaces of holes led to the integral equations for the body force densities which were solved by means of the Laurent series expansion. The results of the above last two papers are of series form and the formulations become extremely cumbersome where only a few non-uniformly distributed holes are involved. The multiple hole–crack interaction problem was the subject of study by Hu et al. (1993). They modeled the holes and cracks, respectively, as unknown pseudo-tractions and unknown distributions of dislocations, on the surface of these defects. The ensuing integral equations on cracks were of Cauchy singular type whereas those on the holes were of second order Fredholm kind. The numerical solution of these equations led to the stress intensity factor at crack tips.

In this study the edge dislocation solution is utilized to derive Cauchy singular integral equations for an infinite plane weakened by arbitrarily oriented curved cracks and cavities. Cavities are modeled as closed cracks without singularity. The integral equations are converted to hypersingular equations in terms of unknown displacement components of crack edges. The series expansions of displacement components are used to solve the equations. The mode I and II stress intensity factors for cracks and hoop stress for cavities are obtained for several examples.

2. Formulation

We consider an infinite orthotropic plane and take the coordinate axes in the directions of material orthotropy. The stress analysis in the plane weakened by a climb and glide edge dislocations was carried out by Faal and Fariborz (2007). To render the article complete the dislocation solution in the infinite plane is restated here. The stress fields caused by a climb and a glide dislocations with Bergers vectors, B_x and B_y, respectively, where the coordinate axes are the axes of principal material orthotropy are

$$\begin{Bmatrix} \sigma_x \\ \sigma_y \\ \sigma_{xy} \end{Bmatrix} = \frac{E_x}{2\pi(r_1+r_2)(r_1^2y^2+x^2)(r_2^2y^2+x^2)} \times \left[B_x \begin{Bmatrix} y\left[(r_1^2+r_2^2+r_1r_2)x^2+(r_1r_2)^2y^2\right] \\ y(r_1r_2y^2-x^2) \\ x(r_1r_2y^2-x^2) \end{Bmatrix} - \frac{B_y}{r_1r_2} \begin{Bmatrix} r_1r_2x(x^2-r_1r_2y^2) \\ x\left[x^2+(r_1^2+r_2^2+r_1r_2)y^2\right] \\ r_1r_2y(x^2-r_1r_2y^2) \end{Bmatrix} \right]. \tag{1}$$

The constants in Eq. (1), for the plane stress situation

$$\begin{aligned} r_1 &= \sqrt{\left(\frac{E_x}{2G_{xy}}-\nu_{xy}\right)+\sqrt{\left(\frac{E_x}{2G_{xy}}-\nu_{xy}\right)^2-\frac{E_x}{E_y}}}, \\ r_2 &= \sqrt{\left(\frac{E_x}{2G_{xy}}-\nu_{xy}\right)-\sqrt{\left(\frac{E_x}{2G_{xy}}-\nu_{xy}\right)^2-\frac{E_x}{E_y}}} \end{aligned} \tag{2}$$

are real and positive (Lekhnitskii, 1963). The dislocation solutions may be employed to analyze infinite planes with several defects. The defects are considered as cracks and cavities while cavities are simulated as closed curved cracks without singularity. Let climb and glide dislocations with densities b_x and b_y, respectively, be distributed on the surface of a crack. The stress fields caused at a point by the above-mentioned distribution of dislocations employing Eq. (1) become

$$\begin{Bmatrix} \sigma_x(x,y) \\ \sigma_y(x,y) \\ \sigma_{xy}(x,y) \end{Bmatrix} = \frac{E_x}{2\pi(r_1+r_2)} \int_{-1}^{1} \frac{\sqrt{[\alpha'(t)]^2+[\beta'(t)]^2}}{[(r_1(y-\beta))^2+(x-\alpha)^2][(r_2(y-\beta))^2+(x-\alpha)^2]}$$
$$\times \left\{ b_x(t) \begin{Bmatrix} (y-\beta)[(r_1^2+r_2^2+r_1r_2)(x-\alpha)^2+(r_1r_2)^2(y-\beta)^2] \\ (y-\beta)[r_1r_2(y-\beta)^2-(x-\alpha)^2] \\ (x-\alpha)[r_1r_2(y-\beta)^2-(x-\alpha)^2] \end{Bmatrix} \right.$$
$$\left. -\frac{1}{r_1r_2} b_y(t) \begin{Bmatrix} r_1r_2(x-\alpha)[(x-\alpha)^2-r_1r_2(y-\beta)^2] \\ (x-\alpha)[(r_1^2+r_2^2+r_1r_2)(y-\beta)^2+(x-\alpha)^2] \\ r_1r_2(y-\beta)[(x-\alpha)^2-r_1r_2(y-\beta)^2] \end{Bmatrix} \right\} \mathrm{d}t \tag{3}$$

In Eq. (3), $(\alpha(t),\beta(t))$, $-1 \leqslant t \leqslant 1$, specify the geometry of the crack with respect to the coordinate system (x,y) and prime denotes differentiation with respect to the relevant argument. The moveable orthogonal coordinates (s,n) are chosen such that the origin may move on a defect while s-axis remains tangent to the defect surface. The components of stress and dislocation density may be transformed to (s,n) coordinates

$$\begin{aligned}
\sigma_n &= \frac{\sigma_x+\sigma_y}{2} - \frac{\sigma_x-\sigma_y}{2}\cos(2\psi) - \sigma_{xy}\sin(2\psi), \\
\sigma_s &= -\frac{\sigma_x-\sigma_y}{2}\sin(2\psi) + \sigma_{xy}\cos(2\psi), \\
b_x &= b_s\cos(\psi) - b_n\sin(\psi), \\
b_y &= b_s\sin(\psi) + b_n\cos(\psi),
\end{aligned} \tag{4}$$

where $\psi(t) = \tan^{-1}(\beta'/\alpha')$ is the angle between the s and x axes. By employing the principle of superposition the components of traction vector at a point with coordinates $(\alpha_j(\eta),\beta_j(\eta))$, where parameter $-1 \leqslant \eta \leqslant 1$, on the surface of jth defect for a plane weakened by N defects become

$$\begin{aligned}
\sigma_n(\alpha_j(\eta),\beta_j(\eta)) &= \sum_{i=1}^{N}\int_{-1}^{1} k_{11ij}(\eta,t)\sqrt{[\alpha_i'(t)]^2+[\beta_i'(t)]^2}\,b_{si}(t)\,\mathrm{d}t \\
&\quad + \sum_{i=1}^{N}\int_{-1}^{1} k_{12ij}(\eta,t)\sqrt{[\alpha_i'(t)]^2+[\beta_i'(t)]^2}\,b_{ni}(t)\,\mathrm{d}t, \\
\sigma_s(\alpha_j(\eta),\beta_j(\eta)) &= \sum_{i=1}^{N}\int_{-1}^{1} k_{21ij}(\eta,t)\sqrt{[\alpha_i'(t)]^2+[\beta_i'(t)]^2}\,b_{si}(t)\,\mathrm{d}t \\
&\quad + \sum_{i=1}^{N}\int_{-1}^{1} k_{22ij}(\eta,t)\sqrt{[\alpha_i'(t)]^2+[\beta_i'(t)]^2}\,b_{ni}(t)\,\mathrm{d}t, \quad j = 1,2,\ldots,N.
\end{aligned} \tag{5}$$

The kernels in Eq. (5) are

$$\begin{aligned}
k_{11ij}(\eta,t) &= K_{11ij}(\eta,t)\cos\psi_i(t) + K_{12ij}(\eta,t)\sin\psi_i(t), \\
k_{12ij}(\eta,t) &= K_{12ij}(\eta,t)\cos\psi_i(t) - K_{11ij}(\eta,t)\sin\psi_i(t), \\
k_{21ij}(\eta,t) &= K_{21ij}(\eta,t)\cos\psi_i(t) + K_{22ij}(\eta,t)\sin\psi_i(t), \\
k_{22ij}(\eta,t) &= K_{22ij}(\eta,t)\cos\psi_i(t) - K_{21ij}(\eta,t)\sin\psi_i(t),
\end{aligned} \tag{6}$$

where functions in the right-hand side of (6) are

$$
\begin{aligned}
K_{11ij}(\eta,t) = {} & \frac{E_x}{4\pi(r_1+r_2)}\Big\{(\beta_j-\beta_i)[(r_1^2+r_2^2+r_1r_2-1)(\alpha_j-\alpha_i)^2+r_1r_2(r_1r_2+1)(\beta_j-\beta_i)^2] \\
& -(\beta_j-\beta_i)[(r_1^2+r_2^2+r_1r_2+1)(\alpha_j-\alpha_i)^2+r_1r_2(r_1r_2-1)(\beta_j-\beta_i)]\cos(2\psi_j) \\
& -2(\alpha_j-\alpha_i)[r_1r_2(\beta_j-\beta_i)^2-(\alpha_j-\alpha_i)^2]\sin(2\psi_j)\Big\}/[(r_1(\beta_j-\beta_i))^2 \\
& +(\alpha_j-\alpha_i)^2][(r_2(\beta_j-\beta_i))^2+(\alpha_j-\alpha_i)^2], \\
K_{12ij}(\eta,t) = {} & -\frac{E_x}{4\pi(r_1+r_2)}\Big\{(\alpha_j-\alpha_i)[(r_1^2+r_2^2+r_1r_2(1-r_1r_2))(\beta_j-\beta_i)^2-(1+r_1r_2)(\alpha_j-\alpha_i)^2] \\
& +(\alpha_j-\alpha_i)[(r_1^2+r_2^2+r_1r_2(1+r_1r_2))(\beta_j-\beta_i)^2+(1-r_1r_2)(\alpha_j-\alpha_i)^2]\cos(2\psi_j) \\
& +2r_1r_2(\beta_j-\beta_i)[r_1r_2(\beta_j-\beta_i)^2-(\alpha_j-\alpha_i)^2]\sin(2\psi_j)\Big\}/[(r_1(\beta_j-\beta_i))^2 \\
& +(\alpha_j-\alpha_i)^2][(r_2(\beta_j-\beta_i))^2+(\alpha_j-\alpha_i)^2], \\
K_{21ij}(\eta,t) = {} & \frac{E_x}{4\pi(r_1+r_2)}\Big\{2(\alpha_j-\alpha_i)[r_1r_2(\beta_j-\beta_i)^2-(\alpha_j-\alpha_i)^2]\cos(2\psi_j) \\
& -(\beta_j-\beta_i)[(r_1^2+r_2^2+r_1r_2+1)(\alpha_j-\alpha_i)^2+r_1r_2(r_1r_2-1)(\beta_j-\beta_i)^2]\sin(2\psi_j)\Big\}/[(r_1(\beta_j-\beta_i))^2 \\
& +(\alpha_j-\alpha_i)^2][(r_2(\beta_j-\beta_i))^2+(\alpha_j-\alpha_i)^2], \\
K_{22ij}(\eta,t) = {} & \frac{E_x}{4\pi r_1r_2(r_1+r_2)}\Big\{2r_1r_2[r_1r_2(\beta_j-\beta_i)^2-(\alpha_j-\alpha_i)^2][(\beta_j-\beta_i)\cos(2\psi_j) \\
& -(\alpha_j-\alpha_i)[(r_1^2+r_2^2+r_1r_2(1+r_1r_2))(\beta_j-\beta_i)^2+(1-r_1r_2)(\alpha_j-\alpha_i)^2]\sin(2\psi_j)\Big\}/[(r_1(\beta_j-\beta_i))^2 \\
& +(\alpha_j-\alpha_i)^2][(r_2(\beta_j-\beta_i))^2+(\alpha_j-\alpha_i)^2]. \qquad (7)
\end{aligned}
$$

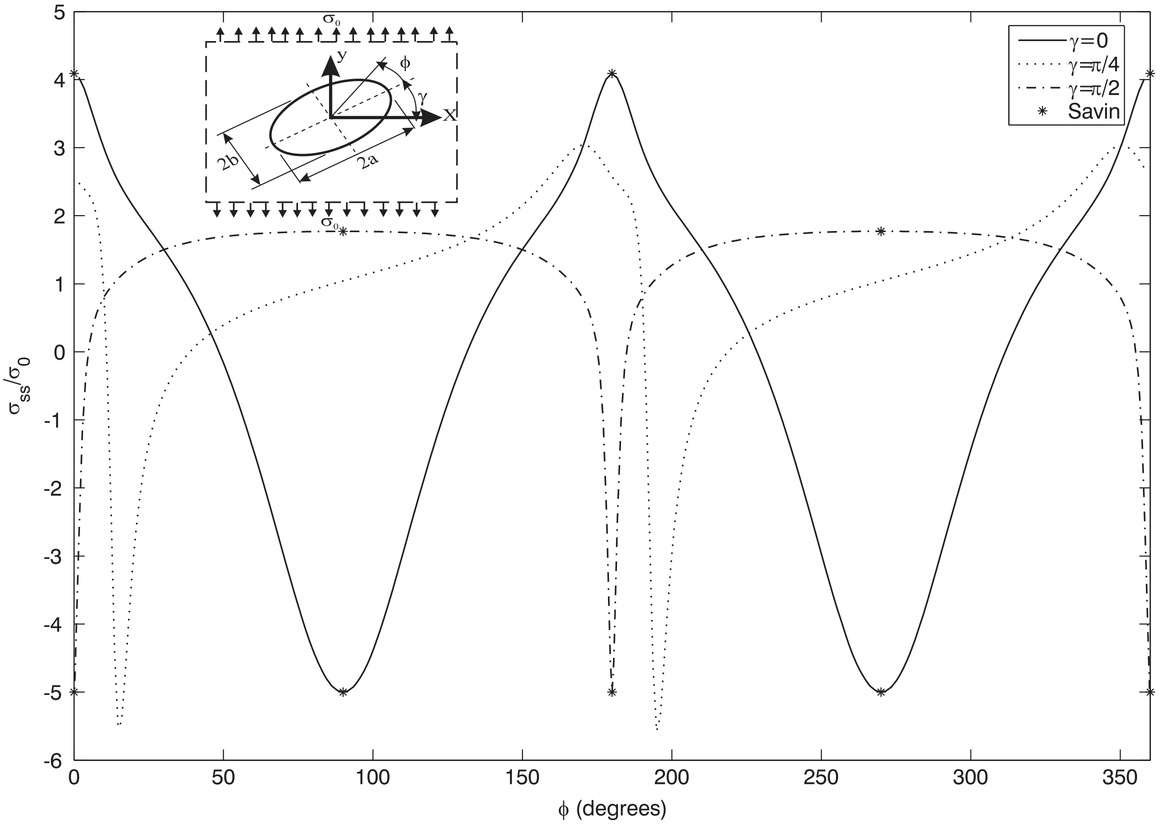

Fig. 1. Dimensionless hoop stress for elliptical cavity.

We should emphasize that in Eq. (7) quantities with subscript i are functions of t, whereas the same quantities with subscript j are functions of η. The kernels in (5) exhibit Cauchy type singularity for $i = j$ as $t \to \eta$. To extract the singular terms the Taylor series expansion of $\alpha_j(t)$ and $\beta_j(t)$ in the vicinity of η is plugged into Eq. (7) yielding

$$\begin{aligned} K_{11jj}(\eta,t) &= \frac{a_{11,-1j}}{\eta - t} + \sum_{m=0}^{\infty} a_{11,mj}(\eta - t)^m, \\ K_{12jj}(\eta,t) &= \frac{a_{12,-1j}}{\eta - t} + \sum_{m=0}^{\infty} a_{12,mj}(\eta - t)^m, \\ K_{21jj}(\eta,t) &= \frac{a_{21,-1j}}{\eta - t} + \sum_{m=0}^{\infty} a_{21,mj}(\eta - t)^m, \\ K_{22jj}(\eta,t) &= \frac{a_{22,-1j}}{\eta - t} + \sum_{m=0}^{\infty} a_{22,mj}(\eta - t)^m. \end{aligned} \tag{8}$$

The coefficients of singular terms are given in Appendix A. The coefficients of regular terms are functions of η and do not take part in the ensuing analysis. Employing the definition of dislocation density function, the climb and glide dislocation density functions b_x and b_y, respectively, for a typical defect in terms of the components of displacement on the defect Δu_x and Δu_y may be written as

$$\begin{aligned} b_x(t) &= \frac{\Delta u_x'(t)}{\sqrt{[\alpha'(t)]^2 + [\beta'(t)]^2}}, \\ b_y(t) &= \frac{\Delta u_y'(t)}{\sqrt{[\alpha'(t)]^2 + [\beta'(t)]^2}}. \end{aligned} \tag{9}$$

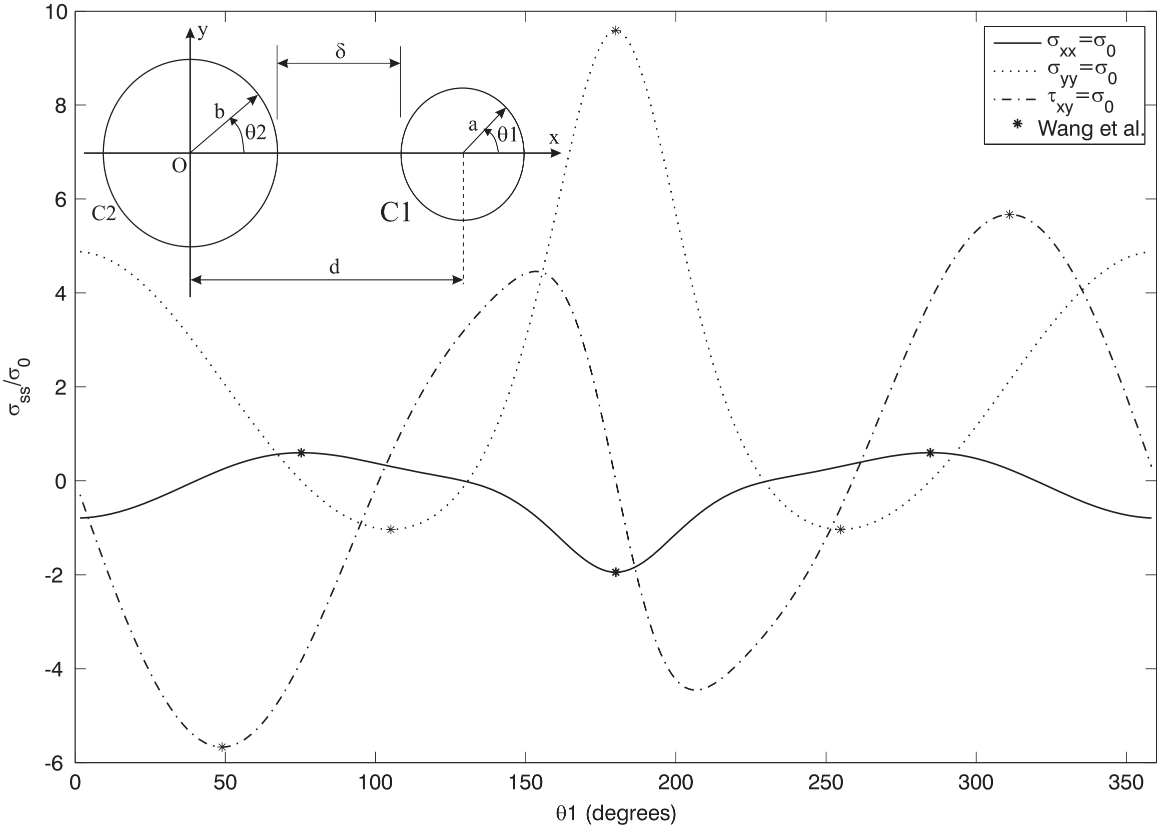

Fig. 2. Dimensionless hoop stress for C_1 cavity.

The components of displacement in the two coordinate systems (x,y) and (n,s) are related by

$$\begin{aligned}\Delta u_x &= \Delta u_s\cos(\psi) - \Delta u_n\sin(\psi),\\ \Delta u_y &= \Delta u_s\sin(\psi) + \Delta u_n\cos(\psi).\end{aligned} \tag{10}$$

The derivative of above equations is readily known

$$\begin{aligned}\Delta u'_x &= \Delta u'_s\cos(\psi) - \Delta u'_n\sin(\psi) - (\Delta u_s\sin(\psi) + \Delta u_n\cos(\psi))\psi',\\ \Delta u'_y &= \Delta u'_s\sin(\psi) + \Delta u'_n\cos(\psi) + (\Delta u_s\cos(\psi) - \Delta u_n\sin(\psi))\psi'.\end{aligned} \tag{11}$$

Substituting (9) and (11) into the last two of (4) and solving the resultant equations for b_s and b_n, the dislocation density functions for the ith defect in (n,s) coordinates result in

$$\begin{aligned}b_{si}(t) &= \frac{1}{\sqrt{[\alpha'_i(t)]^2 + [\beta'_i(t)]^2}}[\Delta u'_{si}(t) - \psi'_i(t)\Delta u_{ni}(t)],\\ b_{ni}(t) &= \frac{1}{\sqrt{[\alpha'_i(t)]^2 + [\beta'_i(t)]^2}}[\Delta u'_{ni}(t) + \psi'_i(t)\Delta u_{si}(t)].\end{aligned} \tag{12}$$

In order to circumvent the difficulties which may be encountered in the numerical solution of Cauchy singular integral Eq. (5) for cavities, we substitute Eqs. (12) into (5) use, formally, the integration by parts together with the closure requirement i.e., $\Delta u_{ki}(-1) = \Delta u_{ki}(1) = 0$, $k = n, s$, $i = 1, 2, \ldots, N$, and arrive at the following system of hypersingular integral equations:

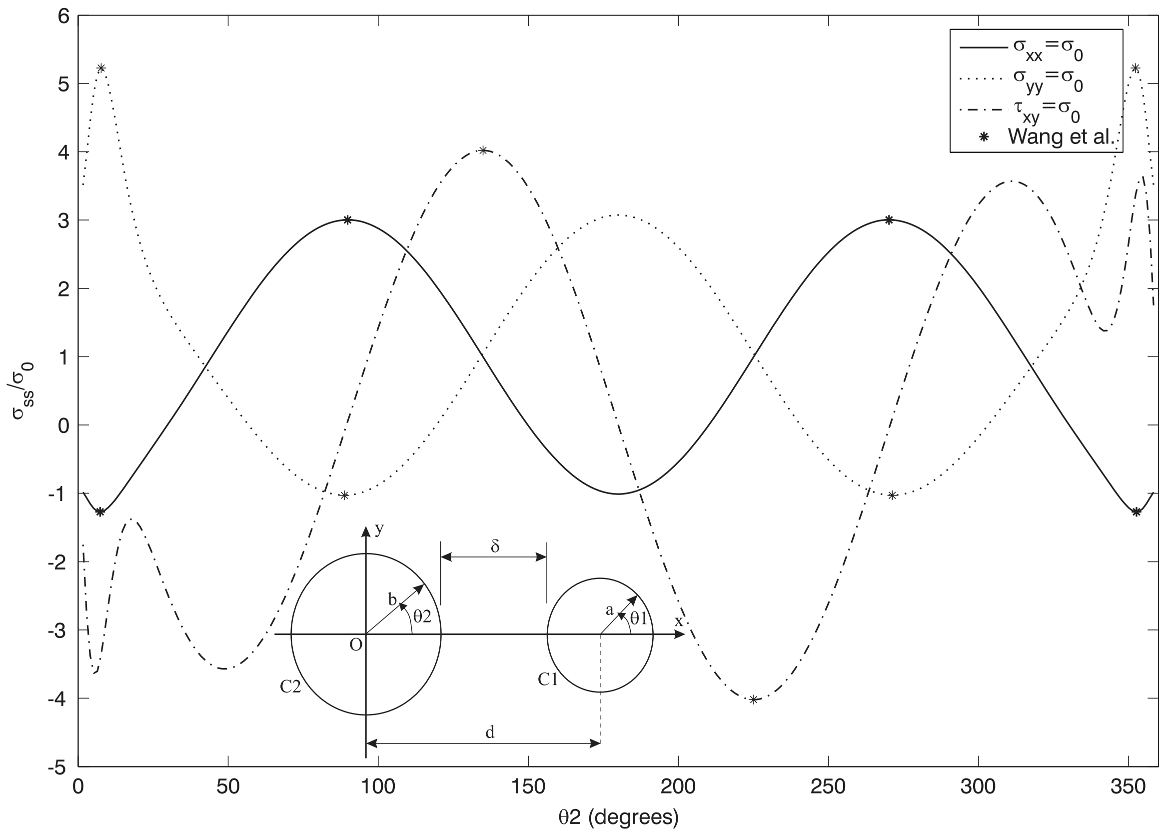

Fig. 3. Dimensionless hoop stress for C_2 cavity.

$$\begin{aligned}\sigma_n(\alpha_j(\eta),\beta_j(\eta)) &= \sum_{i=1}^{N}\int_{-1}^{1}k^H_{11ij}(\eta,t)\Delta u_{si}(t)\,\mathrm{d}t + \sum_{i=1}^{N}\int_{-1}^{1}k^H_{12ij}(\eta,t)\Delta u_{ni}(t)\,\mathrm{d}t,\\ \sigma_s(\alpha_j(\eta),\beta_j(\eta)) &= \sum_{i=1}^{N}\int_{-1}^{1}k^H_{21ij}(\eta,t)\Delta u_{si}(t)\,\mathrm{d}t + \sum_{i=1}^{N}\int_{-1}^{1}k^H_{22ij}(\eta,t)\Delta u_{ni}(t)\,\mathrm{d}t, \quad j=1,2,\ldots,N,\end{aligned} \tag{13}$$

where the kernels in Eq. (13) are

$$\begin{aligned}k^H_{11ij}(\eta,t) &= k_{12ij}(\eta,t)\psi_i'(t) - \frac{\partial k_{11ij}(\eta,t)}{\partial t},\\ k^H_{12ij}(\eta,t) &= -k_{11ij}(\eta,t)\psi_i'(t) - \frac{\partial k_{12ij}(\eta,t)}{\partial t},\\ k^H_{21ij}(\eta,t) &= k_{22ij}(\eta,t)\psi_i'(t) - \frac{\partial k_{21ij}(\eta,t)}{\partial t},\\ k^H_{22ij}(\eta,t) &= -k_{21ij}(\eta,t)\psi_i'(t) - \frac{\partial k_{22ij}(\eta,t)}{\partial t}.\end{aligned} \tag{14}$$

The above equalities contain hypersingular as well as Cauchy singular terms for $i=j$ as $t \to \eta$ and by virtue of (6) may be represented as

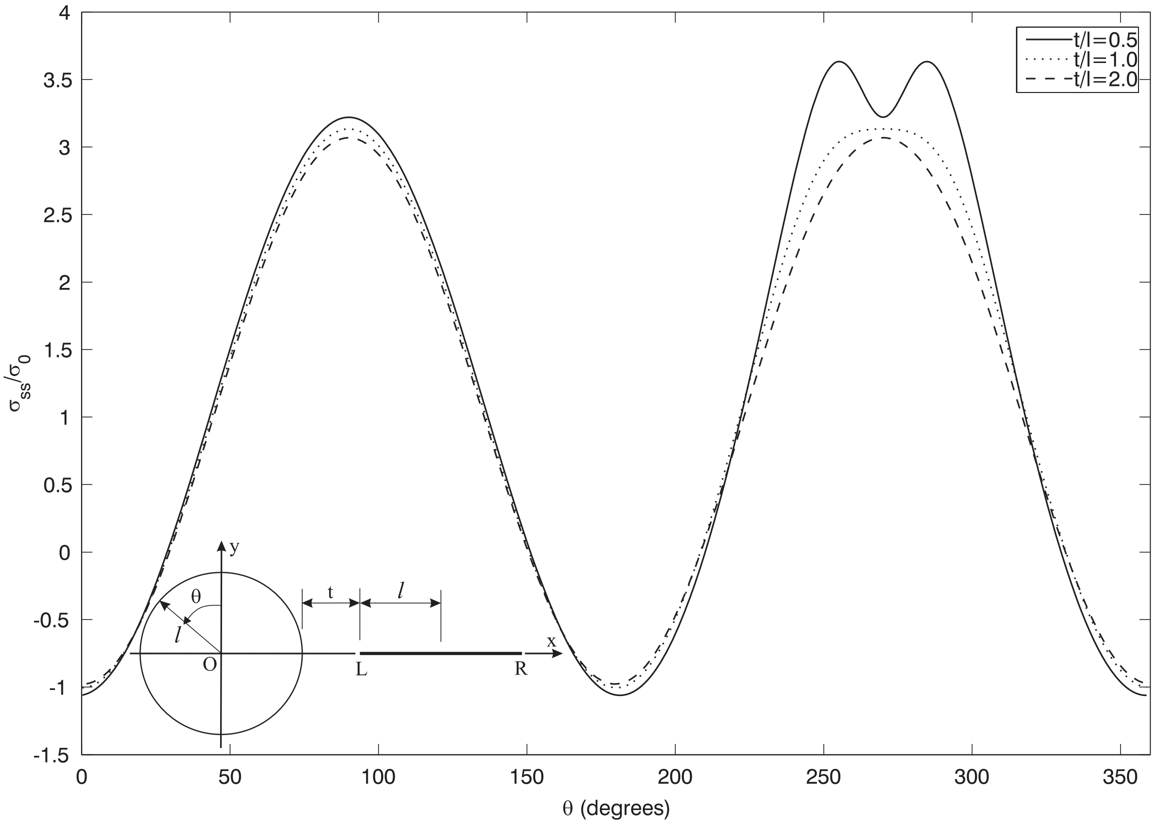

Fig. 4. Dimensionless hoop stress on the cavity in isotropic plane.

$$
\begin{aligned}
k^{H}_{11jj}(\eta,t) &= -\frac{a^{H}_{11,-1j}(\eta)}{(\eta-t)^2} + \frac{a^{H}_{12,-1j}(\eta)}{\eta-t}\psi'_j(\eta) + \sum_{m=0}^{\infty} a^{H}_{11,mj}(\eta-t)^m,\\
k^{H}_{12jj}(\eta,t) &= -\frac{a^{H}_{12,-1j}(\eta)}{(\eta-t)^2} - \frac{a^{H}_{11,-1j}(\eta)}{\eta-t}\psi'_j(\eta) + \sum_{m=0}^{\infty} a^{H}_{12,mj}(\eta-t)^m,\\
k^{H}_{21jj}(\eta,t) &= -\frac{a^{H}_{21,-1j}(\eta)}{(\eta-t)^2} + \frac{a^{H}_{22,-1j}(\eta)}{\eta-t}\psi'_j(\eta) + \sum_{m=0}^{\infty} a^{H}_{21,mj}(\eta-t)^m,\\
k^{H}_{22jj}(\eta,t) &= -\frac{a^{H}_{22,-1j}(\eta)}{(\eta-t)^2} - \frac{a^{H}_{21,-1j}(\eta)}{\eta-t}\psi'_j(\eta) + \sum_{m=0}^{\infty} a^{H}_{22,mj}(\eta-t)^m,
\end{aligned} \tag{15}
$$

where

$$
\begin{aligned}
a^{H}_{11,-1j}(\eta) &= a_{11,-1j}\cos\psi_j(\eta) + a_{12,-1j}\sin\psi_j(\eta),\\
a^{H}_{12,-1j}(\eta) &= a_{12,-1j}\cos\psi_j(\eta) - a_{11,-1j}\sin\psi_j(\eta),\\
a^{H}_{21,-1j}(\eta) &= a_{21,-1j}\cos\psi_j(\eta) + a_{22,-1j}\sin\psi_j(\eta),\\
a^{H}_{22,-1j}(\eta) &= a_{22,-1j}\cos\psi_j(\eta) - a_{21,-1j}\sin\psi_j(\eta).
\end{aligned} \tag{16}
$$

The coefficients $a_{mn,-1j}$, $m,n=1,2$ are those specified in Appendix A. The series in (15) are regular and the coefficients $a^{H}_{kl,mj}, k,l=1,2$ are too lengthy to be given here. Utilizing the Bueckner's principle, the left-hand sides of Eq. (13), with opposite sign, are the traction caused by external loading in the infinite plane without defects on the presumed surfaces of defects. The applied tractions at the far-field σ^{∞}_{x}, σ^{∞}_{y}, σ^{∞}_{xy} are considered to be uniform. Therefore, the left-hand sides of Eq. (13) yield

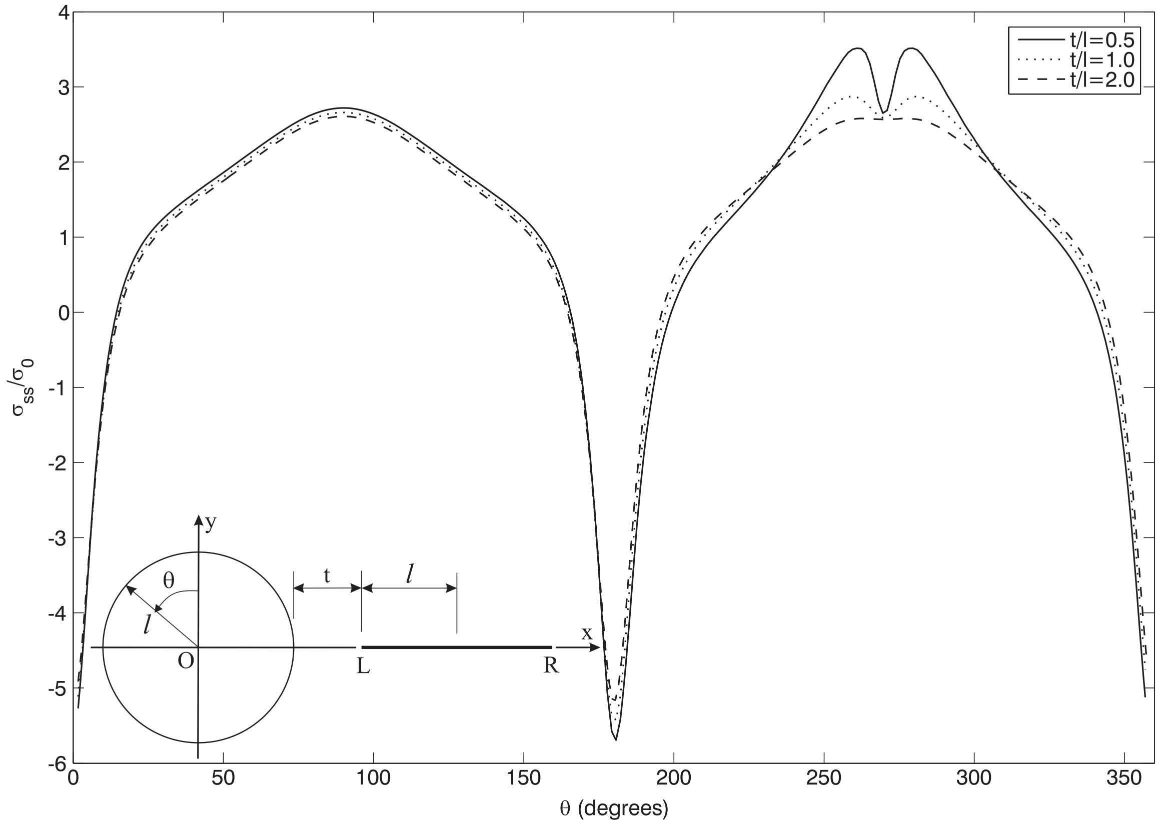

Fig. 5. Dimensionless hoop stress on the cavity in orthotropic plane.

$$\sigma_{nj} = -\frac{\sigma_x^\infty + \sigma_y^\infty}{2} + \frac{\sigma_x^\infty - \sigma_y^\infty}{2}\cos(2\psi_j) + \sigma_{xy}^\infty \sin(2\psi_j),$$
$$\sigma_{sj} = \frac{\sigma_x^\infty - \sigma_y^\infty}{2}\sin(2\psi_j) - \sigma_{xy}^\infty\cos(2\psi_j), \quad j = 1, 2, ..., N. \tag{17}$$

The singular parts of the kernels in integral Eq. (13) should be separated from the regular part. Eq. (13) in light of (15) may be rewritten as

$$\begin{aligned}
\sigma_n(\alpha_j(\eta),\beta_j(\eta)) = {} & -a^H_{11,-1j}(\eta)\int_{-1}^{1}\frac{\Delta u_{sj}(t)}{(\eta-t)^2}\mathrm{d}t - a^H_{12,-1j}(\eta)\int_{-1}^{1}\frac{\Delta u_{nj}(t)}{(\eta-t)^2}\mathrm{d}t + a^H_{12,-1j}(\eta)\psi_j'(\eta)\int_{-1}^{1}\frac{\Delta u_{sj}(t)}{\eta-t}\mathrm{d}t - a^H_{11,-1j}(\eta)\psi_j'(\eta)\int_{-1}^{1}\frac{\Delta u_{nj}(t)}{\eta-t}\mathrm{d}t \\
& + \int_{-1}^{1}[\frac{a^H_{11,-1j}(\eta)}{(\eta-t)^2} - \frac{a^H_{12,-1j}(\eta)}{\eta-t}\psi_j'(\eta) + k^H_{11jj}(\eta,t)]\Delta u_{sj}(t)\,\mathrm{d}t + \int_{-1}^{1}[\frac{a^H_{12,-1j}(\eta)}{(\eta-t)^2} + \frac{a^H_{11,-1j}(\eta)}{\eta-t}\psi_j'(\eta) + k^H_{12jj}(\eta,t)]\Delta u_{nj}(t)\,\mathrm{d}t \\
& + \sum_{\substack{i=1\\ i\neq j}}^{N}\int_{-1}^{1}k^H_{11ij}(\eta,t)\Delta u_{si}(t)\,\mathrm{d}t + \sum_{\substack{i=1\\ i\neq j}}^{N}\int_{-1}^{1}k^H_{12ij}(\eta,t)\Delta u_{ni}(t)\,\mathrm{d}t, \\
\sigma_s(\alpha_j(\eta),\beta_j(\eta)) = {} & -a^H_{21,-1j}(\eta)\int_{-1}^{1}\frac{\Delta u_{sj}(t)}{(\eta-t)^2}\mathrm{d}t - a^H_{22,-1j}(\eta)\int_{-1}^{1}\frac{\Delta u_{nj}(t)}{(\eta-t)^2}\mathrm{d}t + a^H_{22,-1j}(\eta)\psi_j'(\eta)\int_{-1}^{1}\frac{\Delta u_{sj}(t)}{\eta-t}\mathrm{d}t - a^H_{21,-1j}(\eta)\psi_j'(\eta)\int_{-1}^{1}\frac{\Delta u_{nj}(t)}{\eta-t}dt \\
& + \int_{-1}^{1}\left[\frac{a^H_{21,-1j}(\eta)}{(\eta-t)^2} - \frac{a^H_{22,-1j}(\eta)}{\eta-t}\psi_j'(\eta) + k^H_{21jj}(\eta,t)\right]\Delta u_{sj}(t)\,\mathrm{d}t + \int_{-1}^{1}\left[\frac{a^H_{22,-1j}(\eta)}{(\eta-t)^2} + \frac{a^H_{21,-1j}(\eta)}{\eta-t}\psi_j'(\eta) + k^H_{22jj}(\eta,t)\right]\Delta u_{nj}(t)\,\mathrm{d}t \\
& + \sum_{\substack{i=1\\ i\neq j}}^{N}\int_{-1}^{1}k^H_{21ij}(\eta,t)\Delta u_{si}(t)\,\mathrm{d}t + \sum_{\substack{i=1\\ i\neq j}}^{N}\int_{-1}^{1}k^H_{22ij}(\eta,t)\Delta u_{ni}(t)\,\mathrm{d}t, \quad j=1,2,...,N.
\end{aligned} \tag{18}$$

It is worth mentioning that in the right-hand sides of Eq. (18) the first two terms are hypersingular the next two terms are Cauchy singular and the remaining terms are regular in the domain of integration.

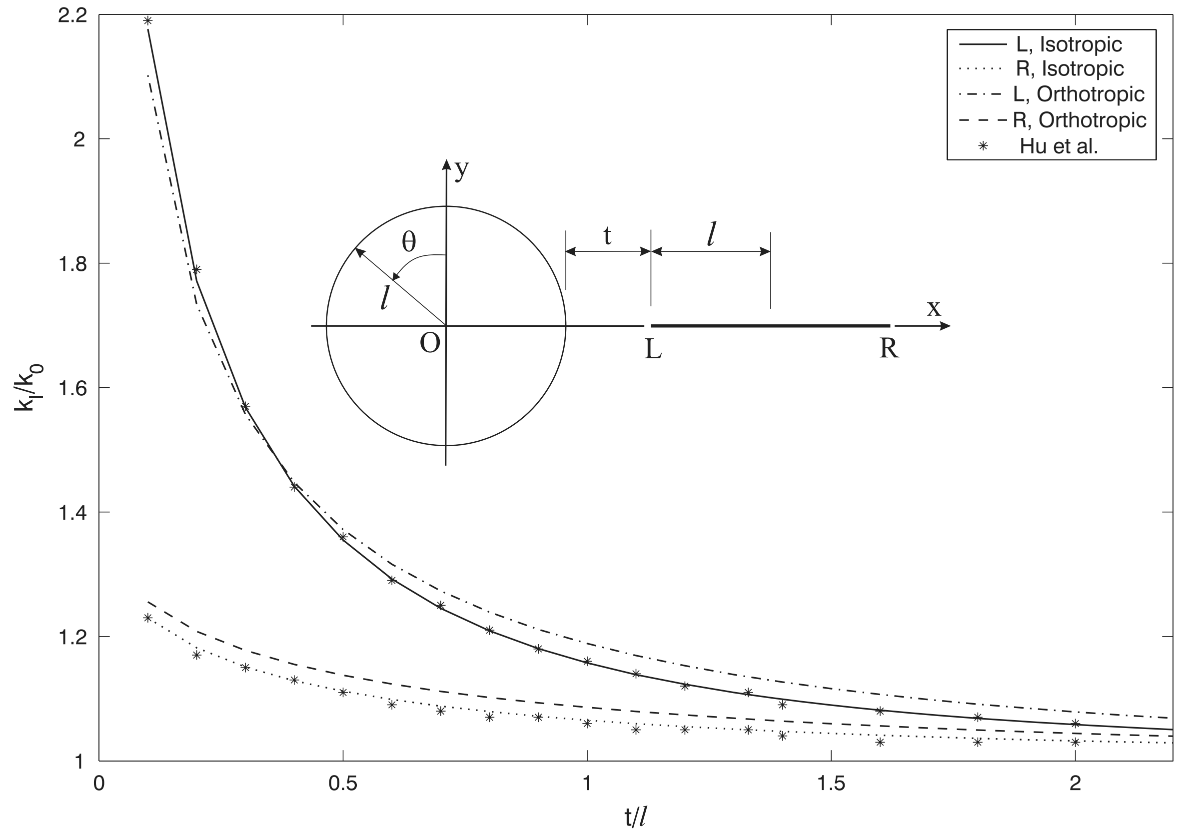

Fig. 6. Crack stress intensity factors in isotropic and orthotropic planes.

3. Solution of integral equations

The numerical solution of Eq. (18) is carried out by the technique devised by Kaya and Erdogan (1987). Let N_1 be the number of cracks and N_2 the number of cavities in the infinite plane. Thus, the total number of defects is $N = N_1 + N_2$. The stress fields near a crack tip in orthotropic materials have the singularity of $1/\sqrt{r}$, where r is the distance from crack tip, see for e.g. Delale (1984). Therefore, the asymptotic behavior of displacement field in the vicinity of crack tip is $\sqrt{r}$ and the crack displacement may be approximated by a truncated series of $M_1 + 1$ terms for each crack as

$$\Delta u_{ki}(t) \cong \sqrt{1-t^2}\sum_{m=0}^{M_1} a_{im}^k U_m(t), \qquad -1 < t < 1, \quad k = n, s, \quad i = 1, 2, \ldots, N_1, \tag{19}$$

where $U_m(t)$ is the Chebyshev polynomial of the second kind. Cavities are considered as closed curved cracks. Thus the stress fields for cavities are bounded and the crack displacement may be evaluated by a series of $M_2 + 1$ terms of Legendre polynomials of first kind as

$$\Delta u_{ki}(t) \cong \sum_{m=0}^{M_2} a_{im}^k P_m(t), \qquad -1 < t < 1, \quad k = n, s, \quad i = N_1 + 1, N_1 + 2, \ldots, N. \tag{20}$$

The substitution of (19) and (20) into the relevant terms of Eq. (18), in conjunction with the application of the following integration formulas:

$$\begin{aligned} &\int_{-1}^{1} \frac{U_m(t)\sqrt{1-t^2}}{(\eta-t)^2}\,\mathrm{d}t = -\pi(m+1)U_m(\eta), &&\int_{-1}^{1} \frac{U_m(t)\sqrt{1-t^2}}{\eta-t}\,\mathrm{d}t = \pi T_{m+1}(\eta) \\ &\int_{-1}^{1} \frac{P_m(t)}{(\eta-t)^2}\,\mathrm{d}t = -\frac{2(m+1)}{1-\eta^2}\left[\eta Q_m(\eta) - Q_{m+1}(\eta)\right], &&\int_{-1}^{1} \frac{P_m(t)}{\eta-t}\,\mathrm{d}t = 2Q_m(\eta), \end{aligned} \tag{21}$$

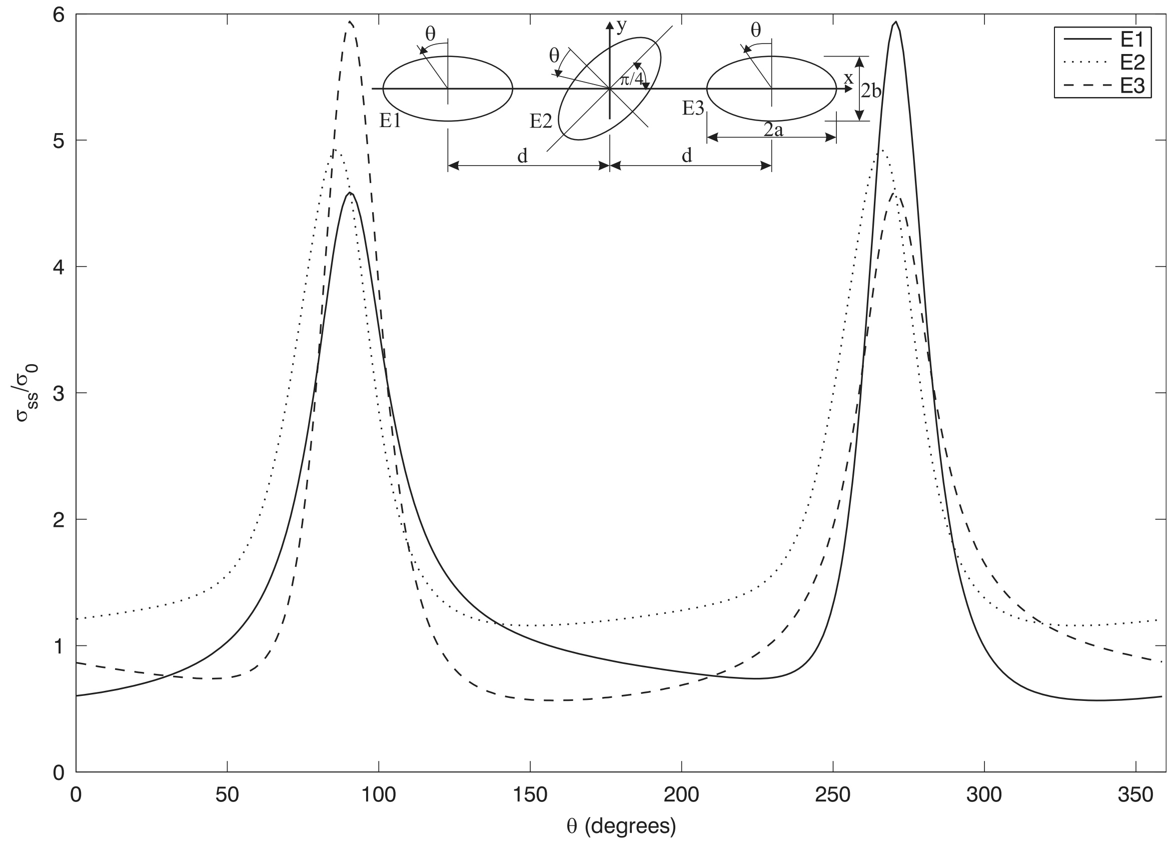

Fig. 7. Dimensionless hoop stress for three elliptical cavities in isotropic planes under far-field biaxial loading.

where $T_m(t)$ is the Chebyshev polynomial of the first kind and $Q_m(t)$ is the Legendre polynomial of second kind, leads to

$$\begin{aligned}
\sigma_n(\alpha_j(\eta),\beta_j(\eta)) = &\sum_{m=0}^{M_1}\{a^s_{jm}[\pi(m+1)a^H_{11,-1j}(\eta)U_m(\eta)+\pi a^H_{12,-1j}(\eta)\psi'_j(\eta)T_{m+1}(\eta)+h_{11jm}(\eta)] \\
&+a^n_{jm}[\pi(m+1)a^H_{12,-1j}(\eta)U_m(\eta)-\pi a^H_{11,-1j}(\eta)\psi'_j(\eta)T_{m+1}(\eta)+h_{12jm}(\eta)]\} \\
&+\sum_{\substack{i=1\\ i\neq j}}^{N_1}\sum_{m=0}^{M_1}\{a^s_{im}h^H_{11ijm}(\eta)+a^n_{im}h^H_{12ijm}(\eta)\}+\sum_{i=N_1+1}^{N}\sum_{m=0}^{M_2}\{a^s_{im}h^H_{11ijm}(\eta)+a^n_{im}h^H_{12ijm}(\eta)\} \\
\sigma_s(\alpha_j(\eta),\beta_j(\eta)) = &\sum_{m=0}^{M_1}\{a^s_{jm}[\pi(m+1)a^H_{21,-1j}(\eta)U_m(\eta)+\pi a^H_{22,-1j}(\eta)\psi'_j(\eta)T_{m+1}(\eta)+h_{21jm}(\eta)] \\
&+a^n_{jm}[\pi(m+1)a^H_{22,-1j}(\eta)U_m(\eta)-\pi a^H_{21,-1j}(\eta)\psi'_j(\eta)T_{m+1}(\eta)+h_{22jm}(\eta)]\} \\
&+\sum_{\substack{i=1\\ i\neq j}}^{N_1}\sum_{m=0}^{M_1}\{a^s_{im}h^H_{21ijm}(\eta)+a^n_{im}h^H_{22ijm}(\eta)\}+\sum_{i=N_1+1}^{N}\sum_{m=0}^{M_2}\{a^s_{im}h^H_{21ijm}(\eta)+a^n_{im}h^H_{22ijm}(\eta)\},\quad j=1,2,\ldots,N_1 \\
\sigma_n(\alpha_j(\eta),\beta_j(\eta)) = &\sum_{m=0}^{M_2}\left\{a^s_{jm}\left[\frac{2(m+1)a^H_{11,-1j}(\eta)}{1-\eta^2}\left[\eta Q_m(\eta)-Q_{m+1}(\eta)\right]+2a^H_{12,-1j}(\eta)\psi'_j(\eta)Q_m(\eta)+h_{11jm}(\eta)\right]\right. \\
&\left.+a^n_{jm}\left[\frac{2(m+1)a^H_{12,-1j}(\eta)}{1-\eta^2}\left[\eta Q_m(\eta)-Q_{m+1}(\eta)\right]-2a^H_{11,-1j}(\eta)\psi'_j(\eta)Q_m(\eta)+h_{12jm}(\eta)\right]\right\} \\
&+\sum_{i=1}^{N_1}\sum_{m=0}^{M_1}\{a^s_{im}h^H_{11ijm}(\eta)+a^n_{im}h^H_{12ijm}(\eta)\}+\sum_{\substack{i=N_1+1\\ i\neq j}}^{N}\sum_{m=0}^{M_2}\{a^s_{im}h^H_{11ijm}(\eta)+a^n_{im}h^H_{12ijm}(\eta)\} \\
\sigma_s(\alpha_j(\eta),\beta_j(\eta)) = &\sum_{m=0}^{M_2}\left\{a^s_{jm}[\frac{2(m+1)a^H_{21,-1j}(\eta)}{1-\eta^2}[\eta Q_m(\eta)-Q_{m+1}(\eta)]+2a^H_{22,-1j}(\eta)\psi'_j(\eta)Q_m(\eta)+h_{21jm}(\eta)]\right. \\
&\left.+a^n_{jm}\left[\frac{2(m+1)a^H_{22,-1j}(\eta)}{1-\eta^2}[\eta Q_m(\eta)-Q_{m+1}(\eta)]-2a^H_{21,-1j}(\eta)\psi'_j(\eta)Q_m(\eta)+h_{22jm}(\eta)\right]\right\} \\
&+\sum_{i=1}^{N_1}\sum_{m=0}^{M_1}\{a^s_{im}h^H_{21ijm}(\eta)+a^n_{im}h^H_{22ijm}(\eta)\} \\
&+\sum_{\substack{i=N_1+1\\ i\neq j}}^{N}\sum_{m=0}^{M_2}\{a^s_{im}h^H_{21ijm}(\eta)+a^n_{im}h^H_{22ijm}(\eta)\},\quad j=N_1+1,N_1+2,\ldots,N.
\end{aligned}\tag{22}$$

The functions in Eq. (22) are

$$\begin{aligned}
h_{11jm}(\eta) &= \int_{-1}^{1}\left[\frac{a^H_{11,-1j}(\eta)}{(\eta-t)^2}-\frac{a^H_{12,-1j}(\eta)}{\eta-t}\psi'_j(\eta)+k^H_{11jj}(\eta,t)\right]W_{jm}(t)\,\mathrm{d}t \\
h_{12jm}(\eta) &= \int_{-1}^{1}\left[\frac{a^H_{12,-1j}(\eta)}{(\eta-t)^2}+\frac{a^H_{11,-1j}(\eta)}{\eta-t}\psi'_j(\eta)+k^H_{12jj}(\eta,t)\right]W_{jm}(t)\,\mathrm{d}t \\
h_{21jm}(\eta) &= \int_{-1}^{1}\left[\frac{a^H_{21,-1j}(\eta)}{(\eta-t)^2}-\frac{a^H_{22,-1j}(\eta)}{\eta-t}\psi'_j(\eta)+k^H_{21jj}(\eta,t)\right]W_{jm}(t)\,\mathrm{d}t \\
h_{22jm}(\eta) &= \int_{-1}^{1}\left[\frac{a^H_{22,-1j}(\eta)}{(\eta-t)^2}+\frac{a^H_{21,-1j}(\eta)}{\eta-t}\psi'_j(\eta)+k^H_{22jj}(\eta,t)\right]W_{jm}(t)\,\mathrm{d}t \\
h^H_{klijm}(\eta) &= \int_{-1}^{1}k^H_{klij}(\eta,t)W_{im}(t)\,\mathrm{d}t,\qquad k,l=1,2,\quad j=1,2,\ldots,N,
\end{aligned}\tag{23}$$

where

$$\begin{aligned} W_{jm}(t) &= U_m(t)\sqrt{1-t^2}, \quad j = 1,2,...,N_1 \\ W_{jm}(t) &= P_m(t), \qquad\qquad j = N_1+1, N_1+2,...,N \end{aligned} \tag{24}$$

The $2N_1 \times (M_1+1) + 2N_2 \times (M_2+1)$ unknown coefficients $a^r_{im}, r = n,s, i = 1,2,...,N_1, m = 0,1,...,M_1$ for cracks and $a^r_{im}, r = n,s, i = N_1+1, N_1+2,...,N, m = 0,1,...,M_2$ for cavities are determined by solving the system of algebraic Eq. (22). The integrations in Eq. (23) for $1 \leqslant j \leqslant N_1$ and $N_1+1 \leqslant j \leqslant N$ are carried out, respectively, by Gauss-Chebychev and Gauss-Legendre quadrature rules. For the sake of numerical expediency, the collocation points η_q, $q = 1,2,\ldots,p_1$ for the first and second Eqs. in (22), are chosen at the middle of Gauss-Chebychev quadrature points, whereas those for the third and fourth equations, η_q, $q = p_1+1, p_1+2,\ldots,p$ are taken at the middle of Gauss-Legendre quadrature points, leading to $2N_1 \times p_1 + 2N_2 \times (p-p_1)$ algebraic equations. Taking $p_1 > M_1+1$, $p - p_1 > M_2+1$, the resultant over-determined system of equations should be solved in the sense of least-squares minimization. The number of terms in series and the number of collocation points on various defects are different. They depend upon the type of defect, crack or cavity, and its interaction with other defects. Nonetheless, sufficient number of collocation points should be taken on a defect to ensure the convergence of the coefficients of the series. For the examples solved in this study, we realized that accurate results may be obtained by taking the number of collocation points about 1.6 times the number of series terms. The displacement fields in the vicinity of crack tips in terms of modes I and II stress intensity factors in anisotropic materials are given in Liebowitz (1968). For orthotropic materials stress intensity factors at the tips of the ith crack in terms of the crack opening displacements reduce to

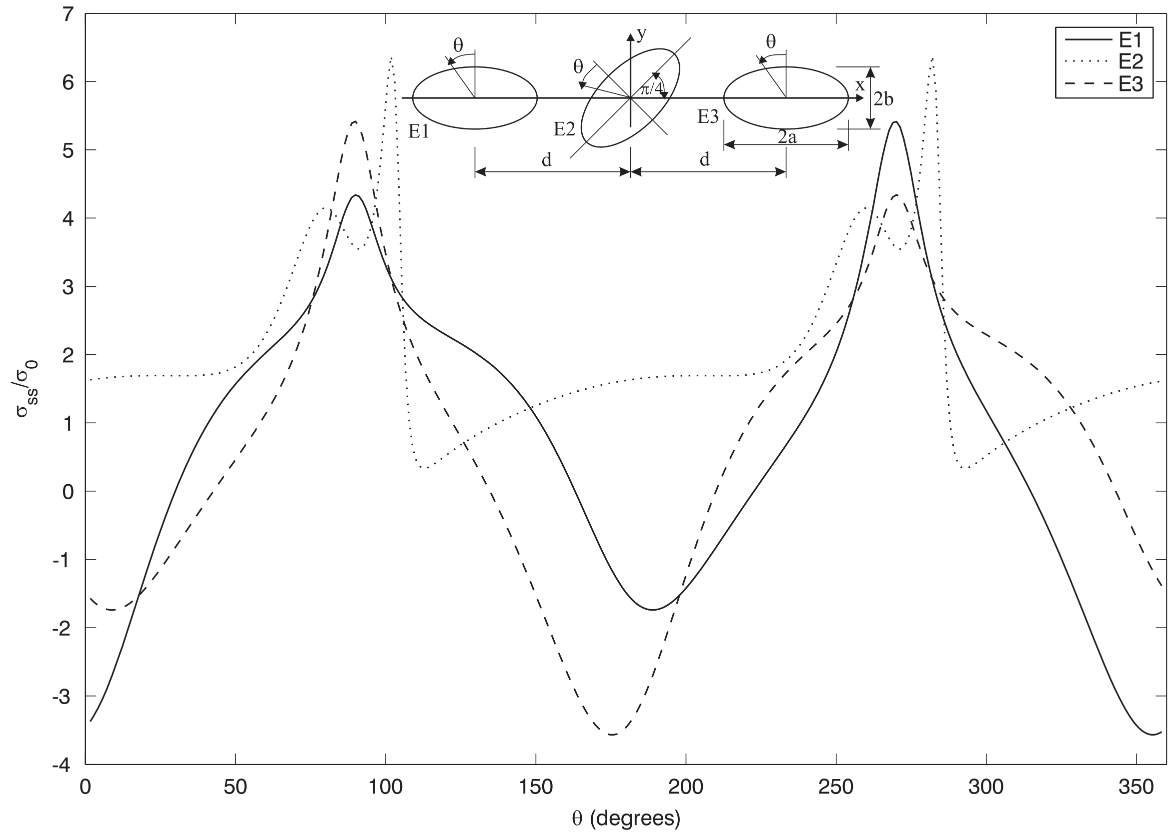

Fig. 8. Dimensionless hoop stress for three elliptical cavities in orthotropic plane under far-field biaxial loading.

$$\begin{Bmatrix} k_{\mathrm{IL}} \\ k_{\mathrm{IIL}} \end{Bmatrix} = \frac{\sqrt{2}E_x}{4(r_1+r_2)} \lim_{r_{\mathrm{L}}\to 0} \frac{1}{\sqrt{r_{\mathrm{L}}}} \begin{Bmatrix} [u_n|_{\theta=\pi} - u_n|_{\theta=-\pi}]/r_1 r_2 \\ u_s|_{\theta=\pi} - u_s|_{\theta=-\pi} \end{Bmatrix},$$
$$\begin{Bmatrix} k_{\mathrm{IR}} \\ k_{\mathrm{IIR}} \end{Bmatrix} = \frac{\sqrt{2}E_x}{4(r_1+r_2)} \lim_{r_{\mathrm{R}}\to 0} \frac{1}{\sqrt{r_{\mathrm{R}}}} \begin{Bmatrix} [u_n|_{\theta=\pi} - u_n|_{\theta=-\pi}]/r_1 r_2 \\ u_s|_{\theta=\pi} - u_s|_{\theta=-\pi} \end{Bmatrix}, \tag{25}$$

where the subscripts L and R, respectively, denote the left and right tips of a crack and the distances of a point on the crack surface from the crack tips are

$$r_{\mathrm{L}} = [(\alpha_i(\eta) - \alpha_i(-1))^2 + (\beta_i(\eta) - \beta_i(-1))^2]^{\frac{1}{2}},$$
$$r_{\mathrm{R}} = [(\alpha_i(\eta) - \alpha_i(1))^2 + (\beta_i(\eta) - \beta_i(1))^2]^{\frac{1}{2}}. \tag{26}$$

Substituting Eqs. (19) and (26) into (25) and using the Taylor series expansion of functions $\alpha_i(\eta)$ and $\beta_i(\eta)$ around the points $\eta = \pm 1$ leads to

$$\begin{Bmatrix} k_{\mathrm{IL}} \\ k_{\mathrm{IIL}} \end{Bmatrix} = \frac{E_x}{2(r_1+r_2)} [[\alpha_i'(-1)]^2 + [\beta_i'(-1)]^2]^{-\frac{1}{4}} \begin{Bmatrix} \sum_{m=0}^{M_1} a_{im}^n U_m(-1)/r_1 r_2 \\ \sum_{m=0}^{M_1} a_{im}^s U_m(-1) \end{Bmatrix},$$
$$\begin{Bmatrix} k_{\mathrm{IR}} \\ k_{\mathrm{IIR}} \end{Bmatrix} = \frac{E_x}{2(r_1+r_2)} [[\alpha_i'(1)]^2 + [\beta_i'(1)]^2]^{-\frac{1}{4}} \begin{Bmatrix} \sum_{m=0}^{M_1} a_{im}^n U_m(1)/r_1 r_2 \\ \sum_{m=0}^{M_1} a_{im}^s U_m(1) \end{Bmatrix}. \tag{27}$$

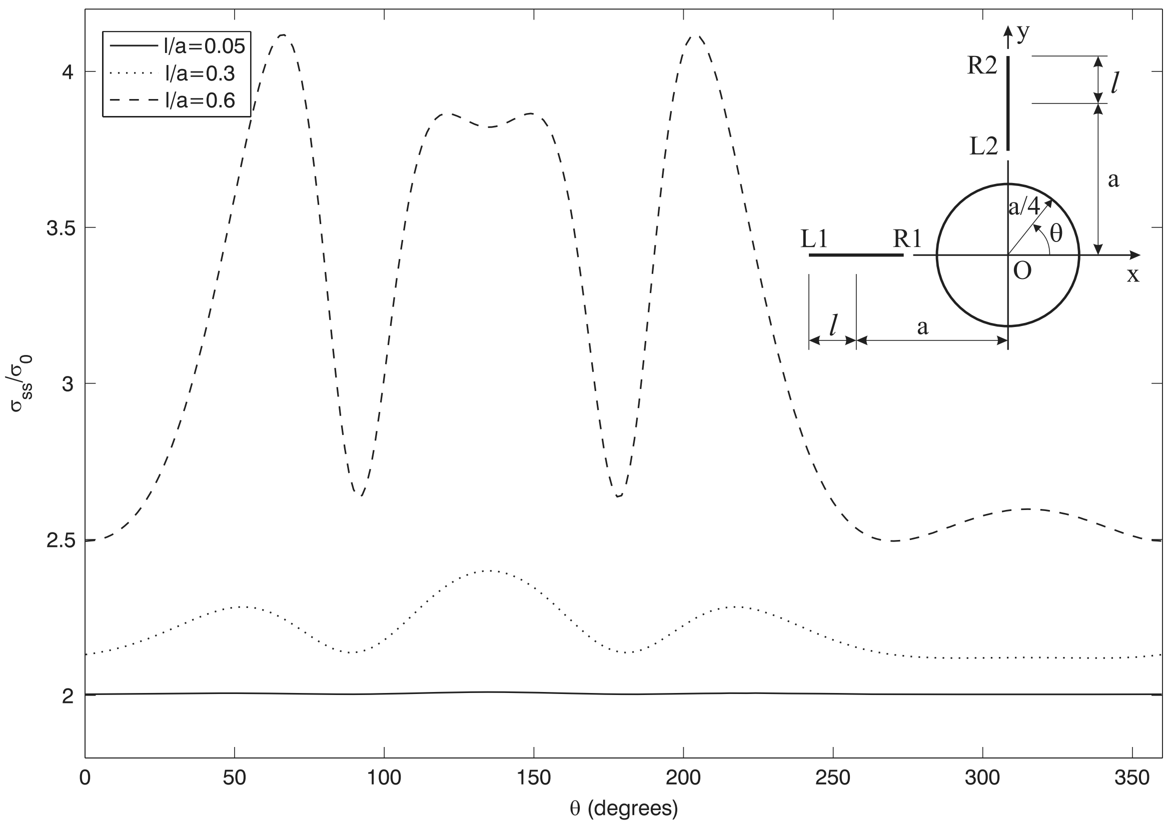

Fig. 9. Dimensionless hoop stress on the cavity in isotropic plane.

Since $U_m(-1) = (-1)^m(m+1)$ and $U_m(1) = (m+1)$, Eq. (27) become

$$\begin{Bmatrix} k_{\mathrm{IL}i} \\ k_{\mathrm{IIL}i} \end{Bmatrix} = \frac{E_x}{2(r_1+r_2)}[[\alpha_i'(-1)]^2 + [\beta_i'(-1)]^2]^{-\frac{1}{4}} \begin{Bmatrix} \sum_{m=0}^{M_1} (-1)^m (m+1) a_{im}^n / r_1 r_2 \\ \sum_{m=0}^{M_1} (-1)^m (m+1) a_{im}^s \end{Bmatrix},$$

$$\begin{Bmatrix} k_{\mathrm{IR}i} \\ k_{\mathrm{IIR}i} \end{Bmatrix} = \frac{E_x}{2(r_1+r_2)}[[\alpha_i'(1)]^2 + [\beta_i'(1)]^2]^{-\frac{1}{4}} \begin{Bmatrix} \sum_{m=0}^{M_1} (m+1) a_{im}^n / r_1 r_2 \\ \sum_{m=0}^{M_1} (m+1) a_{im}^s \end{Bmatrix}, \quad i = 1, 2, \ldots, N_1 \tag{28}$$

On the surface of cavities traction vector vanishes and it is clear that only hoop stress σ_{ss} exists. Consequently, from Hooke's law for orthotropic materials we have

$$\sigma_{ss} = \frac{1}{S_{11}} \varepsilon_{ss}, \tag{29}$$

where the material property S_{11} is in the direction making angle ψ with the x-axis and equals to

$$S_{11} = \frac{1}{E_x}\cos^4(\psi) + \frac{1}{E_y}\sin^4(\psi) + \left(\frac{1}{G_{xy}} - \frac{2v_{xy}}{E_x}\right)\sin^2(\psi)\cos^2(\psi). \tag{30}$$

From the definition of dislocation density function, the first Eq. (12) and Eq. (29) hoop stress on the ith cavity yields

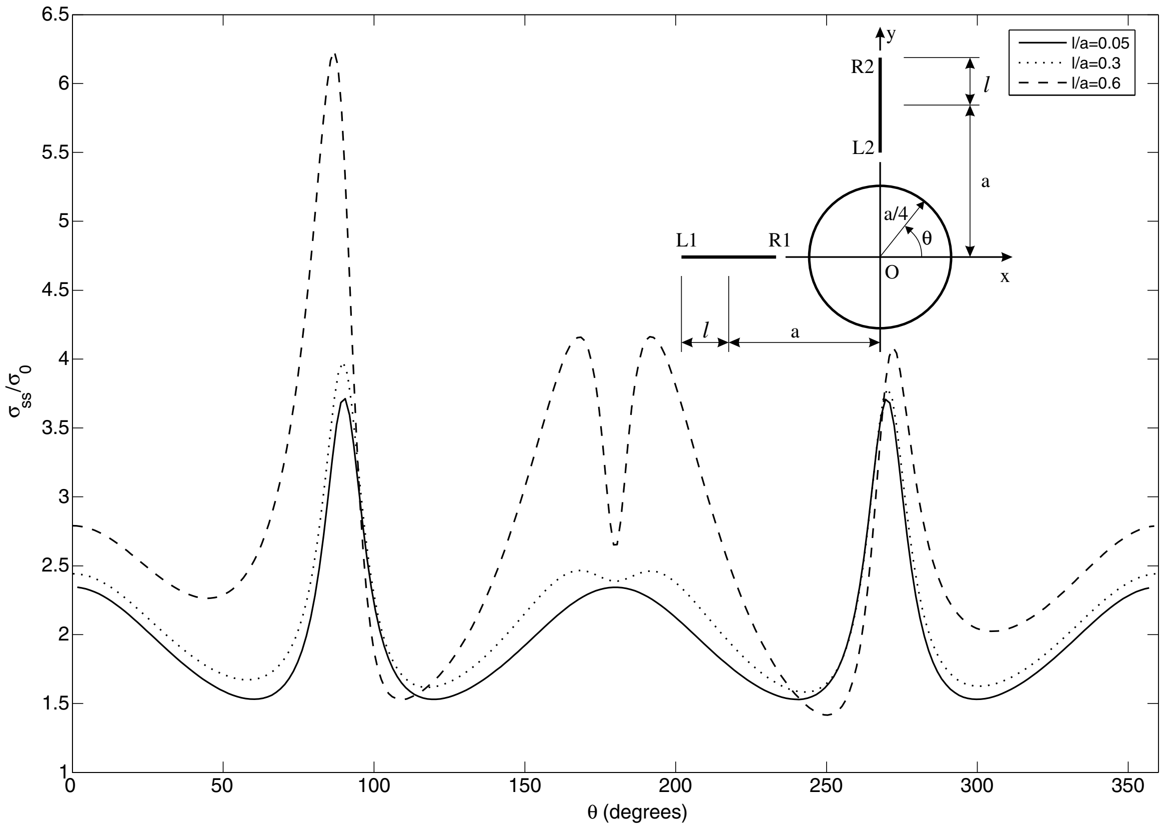

Fig. 10. Dimensionless hoop stress on the cavity in orthotropic plane.

$$\sigma_{ssi}(t) = \frac{1}{S_{11}\sqrt{[\alpha_i'(t)]^2 + [\beta_i'(t)]^2}}[\Delta u_{si}'(t) - \psi_i'(t)\Delta u_{ni}(t)], \quad i = N_1+1, N_1+2, \ldots, N. \tag{31}$$

The substitution of (20) into (31) results in the hoop stress on cavities

$$\sigma_{ssi}(t) = \frac{1}{S_{11}\sqrt{[\alpha_i'(t)]^2 + [\beta_i'(t)]^2}} \sum_{m=0}^{M_2} [(m+1)a_{im}^s \frac{tP_m(t) - P_{m+1}(t)}{1-t^2} - \psi_i'(t)a_{im}^n P_m(t)],$$
$$i = N_1+1, N_1+2, \ldots, N. \tag{32}$$

4. Results and discussion

In all the examples for orthotropic plane, the ratios of moduli of elasticity are $E_y/E_x = 0.04$, $G_{xy}/E_x = 0.02$ and the Poisson's ratio is $v_{xy} = 0.25$. To render the crack stress intensity factors dimensionless the divisor $k_0 = \sigma_0\sqrt{l}$, where σ_0 is the applied traction and l is the half of crack length, is employed. We should also mention that crack closure is not considered in this work. Therefore, the loading and the defects configuration should prevent the possibility of cracks closing. The validity of the analysis is achieved by solving some well known problems in literature. The first problem is an elliptical cavity in the orthotropic medium under far-field uniform tensile traction, $\sigma_y = \sigma_0$. The plots of dimensionless hoop stress for three different orientations of cavity with $a/b = 2$ are drawn in Fig. 1. For $\gamma = 0$, $\pi/2$ the extreme values of hoop stress are identical with the analytical solutions given by Savin (1961). The largest value of hoop stress in the three cases is compressive and occurs where $\gamma = \pi/4$ but not at the vertex of cavity. The second example deals with an isotropic plane

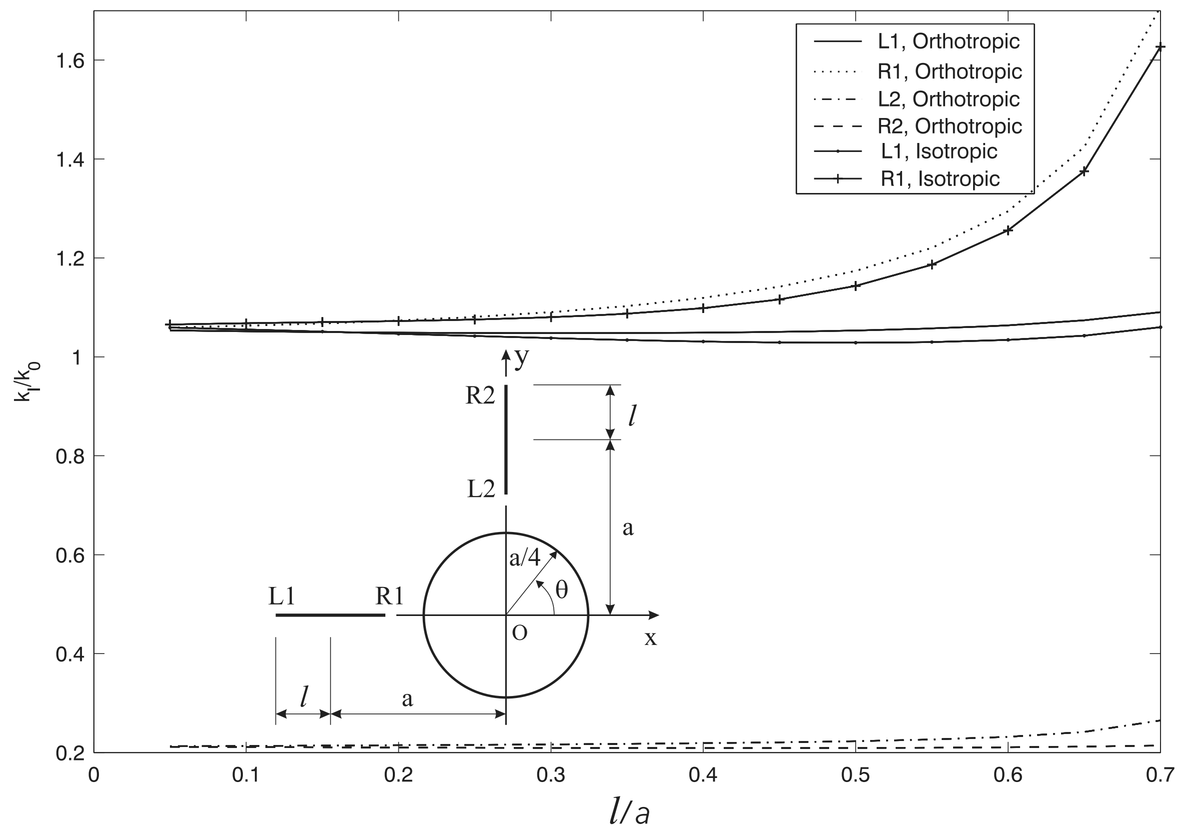

Fig. 11. Mode I stress intensity factor for two cracks in orthotropic plane.

having two circular cavities with the radii a and b separated by distance δ, where $b/a = 5$ and $\delta/a = 0.4$. Three different cases of far-field axial and shear tractions are considered. Figs. 2 and 3 show the nondimensional hoop stress on the cavities C_1 and C_2, respectively. The problem was solved by Wang et al. (2003), utilizing boundary integral method. They reported the maximum and minimum hoop stresses on the cavities which are in good agreement with the results of the present article. As the last check on the analysis, the problem of the infinite isotropic and orthotropic planes weakened by a crack and a circular cavity subjected to uniaxial far-field traction, $\sigma_y = \sigma_0$ is considered. The length of crack is fixed and crack is approaching the cavity. The dimensionless hoop stress on the cavity for three different t/l in isotropic and orthotropic planes is depicted in Figs. 4 and 5, respectively. The variation of hoop stress on the cavity with t/l is not significant. The crack opening i.e., mode I, only occurs. The variation of stress intensity factor with t/l is shown in Fig. 6. The comparison of k/k_0 at the different crack tips reveals that k/k_0 at the crack tip L is higher than at tip R which is due to the stronger interaction with the cavity. The problem for isotropic plane is solved by Isida (1973), employing the method of Laurent series expansion, and latter by Hu et al. (1993) using boundary integral technique. The present solution closely matches with the results of foregoing papers.

The applicability of the methodology developed here is illustrated by solving two new problems. The infinite isotropic and orthotropic planes weakened by three identical elliptical cavities with $a/b = 2$ and $d/b = 5$ are considered. The far-field biaxial traction, $\sigma_x = \sigma_y = \sigma_0$ is applied. The hoop stress on the cavities is shown in Figs. 7 and 8. It is interesting to note that the hoop stress on all cavities in isotropic plane and cavity E_2 in orthotropic material is tensile. In contrast, portions of the cavities E_1 and E_3 in orthotropic media sustain compressive stress. In the second problem a circular cavity and two growing straight cracks is considered. The center of cracks is fixed and far-field constant biaxial traction is applied. The hoop stress on cavity in the isotropic and orthotropic planes for three different l/a is shown in Figs. 9 and 10, respectively. The maximum value of hoop stress for each l/a is larger in orthotropic plane than that in isotropic one. For $l/a = 0.05$,

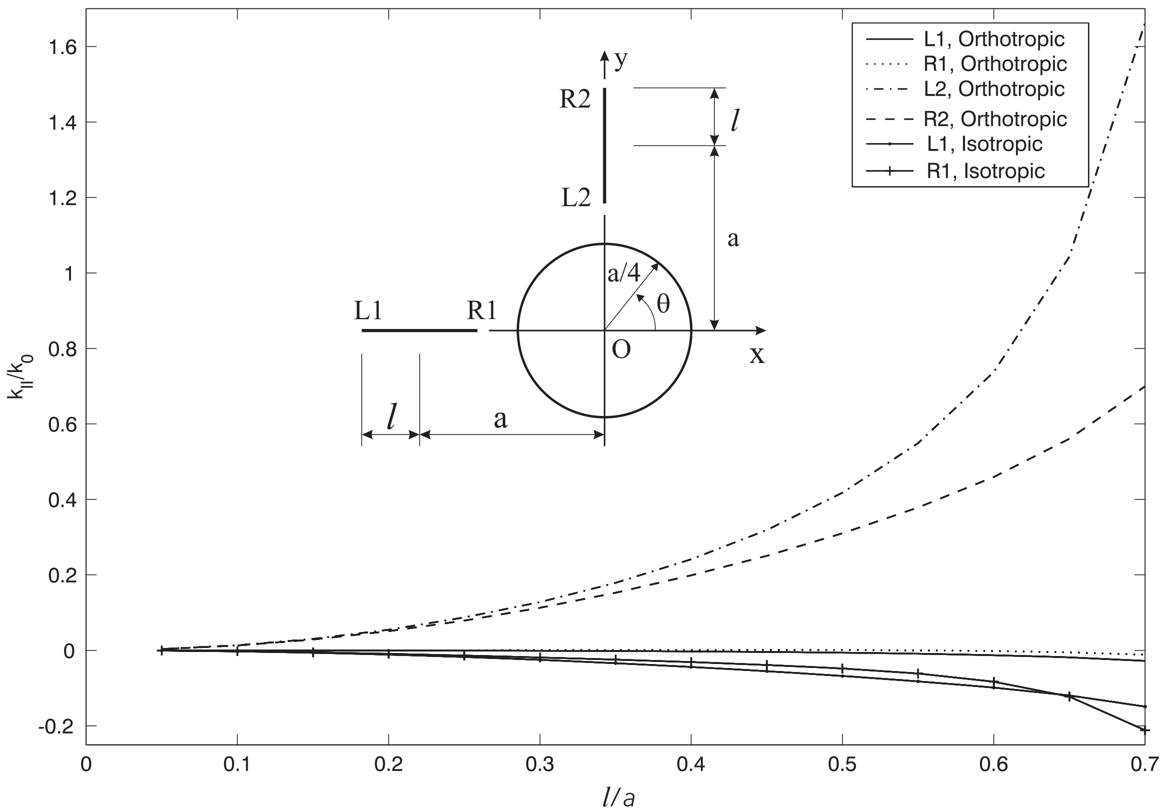

Fig. 12. Mode II stress intensity factor for two cracks in orthotropic plane.

the interaction between cracks and cavity is negligible i.e., cavity in an infinite plane. And the hoop stress on the cavity in the isotropic plane is constant, $\sigma_{ss}/\sigma = 2$, while in the orthotropic plane it varies but is symmetric with respect to the x- and y-axes. The modes I and II stress intensity factors against l/a are shown, respectively, in Figs. 11 and 12. It is noteworthy to mention that in isotopic plane, due to symmetry with respect to the line $\theta = 3\pi/4$, stress intensity factors of two cracks are identical. The comparison of stress intensity factor at different crack tips in orthotropic medium reveals that crack tips with lower k_I/k_0 experience higher k_{II}/k_0.

Appendix A

The coefficients of singular terms in Eq. (8) are

$$\begin{aligned}
a_{11,-1j} = {} & E_x\{\beta_j'[(r_1^2+r_2^2+r_1r_2-1)(\alpha_j')^2+r_1r_2(r_1r_2+1)(\beta_j')^2] \\
& -\beta_j'[(r_1^2+r_2^2+r_1r_2+1)(\alpha_j')^2+r_1r_2(r_1r_2-1)(\beta_j')^2]\cos 2\psi_j-2\alpha_j'[r_1r_2(\beta_j')^2 \\
& -(\alpha_j')^2]\sin 2\psi_j\}/4\pi(r_1+r_2)[(r_1(\beta_j'))^2+(\alpha_j')^2][(r_2(\beta_j'))^2+(\alpha_j')^2], \\
a_{12,-1j} = {} & -E_x\{\alpha_j'[(r_1^2+r_2^2+r_1r_2(1-r_1r_2))(\beta_j')^2-(1+r_1r_2)(\alpha_j')^2] \\
& +\alpha_j'[(r_1^2+r_2^2+r_1r_2(1+r_1r_2))(\beta_j')^2+(1-r_1r_2)(\alpha_j')^2]\cos 2\psi_j+r_1r_2\beta_j'[r_1r_2(\beta_j')^2 \\
& -(\alpha_j')^2]\sin(2\psi_j)\}/4\pi r_1r_2(r_1+r_2)[(r_1(\beta_j'))^2+(\alpha_j')^2][(r_2(\beta_j'))^2+(\alpha_j')^2], \\
a_{21,-1j} = {} & E_x\{2\alpha_j'(r_1r_2(\beta_j')^2-(\alpha_j')^2)\cos 2\psi_j-\beta_j'[(r_1^2+r_2^2+r_1r_2+1)(\alpha_j')^2 \\
& +r_1r_2(r_1r_2-1)(\beta_j')^2]\sin 2\psi_j\}/4\pi(r_1+r_2)[(r_1(\beta_j'))^2+(\alpha_j')^2][(r_2(\beta_j'))^2+(\alpha_j')^2], \\
a_{22,-1j} = {} & E_x\{2r_1r_2\beta_j'(r_1r_2(\beta_j')^2-(\alpha_j')^2)\cos 2\psi_j-\alpha_j'[(r_1^2+r_2^2+r_1r_2(1+r_1r_2))(\beta_j')^2 \\
& +(\alpha_j')^2(1-r_1r_2)]\sin 2\psi_j\}/4\pi r_1r_2(r_1+r_2)[(r_1(\beta_j'))^2+(\alpha_j')^2][(r_2(\beta_j'))^2+(\alpha_j')^2].
\end{aligned}$$

References

Atsumi, A., 1956. On the stresses in a strip under tension and containing two equal circular holes placed longitudinally. Journal of Applied Mechanics 23 (4), 555–562.

Delale, F., 1984. Stress singularities in bonded anisotropic materials. International Journal of Solids and Structures 20 (1), 31–40.

Duan, Z.P., Kienzler, R., Herrmann, G., 1986. An integral equation method and its application to defect mechanics. Journal of Mechanics and Physics of Solids 34 (6), 539–561.

Faal, R.T., Fariborz, S.J., 2007. Stress analysis of orthotropic planes weakened by cracks. Applied Mathematical Modelling, doi:10.1016/j.apm.2006.03.027.

Haddon, R.A., 1967. Stresses in an infinite plate with two unequal circular holes. The Quarterly Journal of Mechanics and Applied Mathematics 20, 277–291.

Howland, R.C.J., 1935. Stresses in a plate containing an infinite row of holes. Proceedings of the Royal Society of London A148, 471–491.

Hu, K.X., Chandra, A., Huang, Y., 1993. Multiple void–crack interaction. International Journal of Solids and Structures 30 (11), 1473–1489.

Isida, M., 1973. Method of laurent series expansion for internal crack problems. In: Sih, G.C. (Ed.), Mechanics of Fracture: Methods of Analysis and Solutions of Crack Problems, vol. 1. Noordhoff, Leyden, pp. 56–130.

Kaya, A.C., Erdogan, F., 1987. On the solution of integral equations with strongly singular kernels. Quarterly of Applied Mathematics 45 (1), 105–122.

Lekhnitskii, S.G., 1963. Theory of Elasticity of an Anisotropic Elastic Body. Holden-Day, San Francisco.

Liebowitz, H., 1968. Fracture Mechanics. Academic Press, New York.

Savin, G.N., 1961. Stress Concentration around Holes. Pergamon Press, New York.

Wang, J., Crouch, S.L., Mogilevskaya, S.G.A., 2003. Complex boundary integral method for multiple circular holes in an infinite plane. Engineering Analysis with Boundary Elements 27, 789–802.